FLUX EFFECT ON THE RADIATION DAMAGE OF AUSTENITIC STEELS

Hygreeva Kiran NAMBURI (CVR)

Centrum výzkumu Řež s.r.o.
Research Centre Rez

This project received funding under the Euratom research and training programme 2014-2018 under grant agreement N° 661913

Review From Previous Presenters

- General Introduction: Internals (M. Serrano)
  - Overview of Internals
  - PWR and BWR internals and their operating conditions
  - Irradiation associated degradation mechanisms in internals
  - Influence on microstructure, Irradiation Embrittlement, Irradiation Creep, IASCC, Wear and Fatigue
- Irradiation effects on internals: microstructure & mechanical properties (B. Tanguy)
  - Definition of upper and lower internals , classification of Austenitic stainless steels as internals (304, 316, 321, 347), irradiation damage in microstructure 304 and 316 SS (low, medium and high flux), influence on mechanical properties.
- Irradiation assisted stress corrosion cracking (A. Hojna)
  - Cases of Field failures of internals, IASCC sensitivity in austenitic steels, threshold dose, RIS, Oxide formation at grain boundary, IASCC mechanism and schematic illustration.

Content

- Introduction
- SOTERIA related work in WP2
- Specimen Preparation
- Results – 321SS/VVER Internals
  - To characterise the effect of **neutron flux** on radiation-induced microstructure.
  - Study the evolution of the **microstructure** with **neutron fluence** including their **role on fracture**
- Summary and conclusions

Introduction

- In order to provide a scientific basis for proposed life extension of current light water reactors, the radiation-induced degradation of stainless steel reactor internals is important.

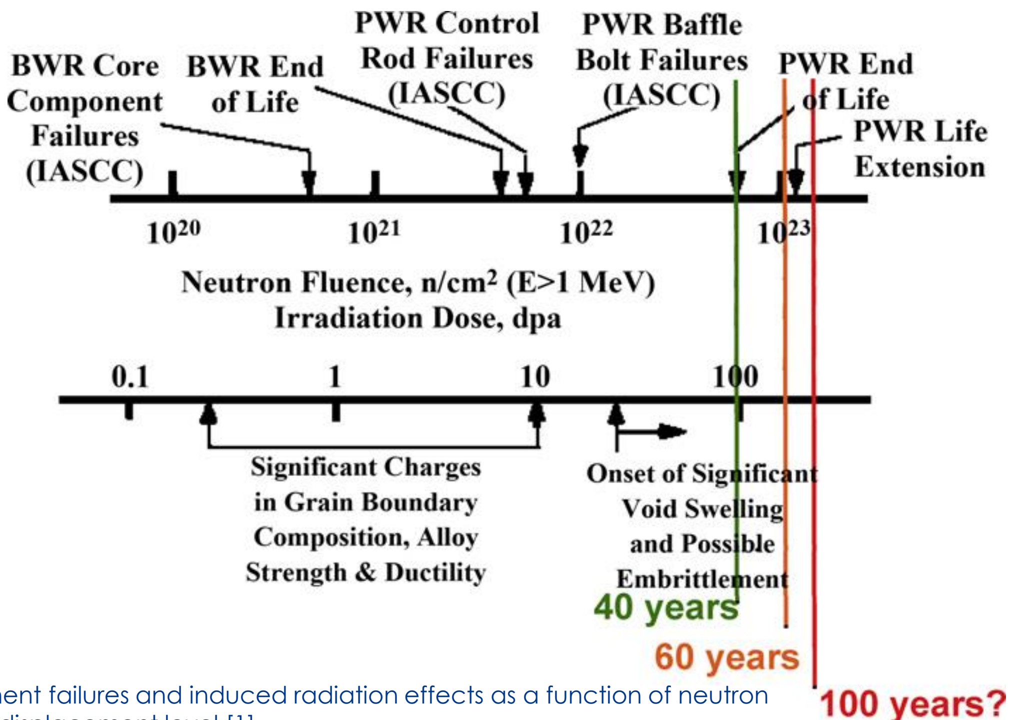

Component failures and induced radiation effects as a function of neutron fluence/displacement level [1]

The 40-year lifetime fluence for reactor core internals in a BWR is $4x10^{22}$ n/cm^2 (E > 1 MeV)
In PWR coresponds to $8 x10^{23}$ n/cm^2 (E > 1 MeV)

Introduction

- The neutron exposition during the nuclear reactor operation results in degradation of microstructural, mechanical and corrosion-mechanical properties of used structural materials.
- Degradation of light-water reactor vessel internals (RVI) made from austenitic stainless steels play a significant role in reactor safety and economical issues.
  - austenitic stainless steels such as 316, 304, 321
  - Internals suffer from high neutron fluence
- The knowledge of properties developed under real service environment is the essential to assess the real state of the material and to predict the degradation of component properties.

Introduction

- In order to investigate the microstructure representative of LTO usually we study materials irradiated at test reactors or at ion irradiation facilities
- To characterize the effects of neutrons on degradation of materials (IASCC)– parts from decomissioned PPs or in-service faulted parts

Cracked RVI-Bolt, WWER-440, Loviisa

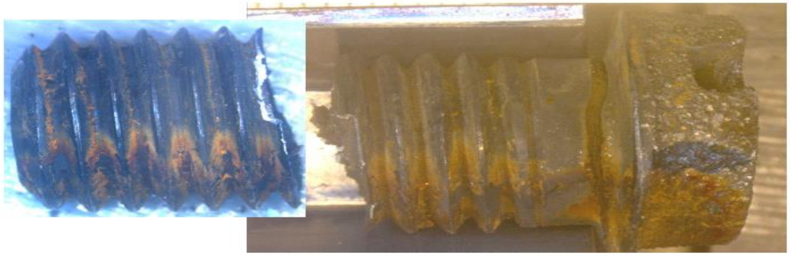

U. Ehrnstén, P. Kytömäki, O. Hietanen. Investigations on core basket bolts from a WWER 440 power plant. Proc. *15th International Conference on Environmental Degradation of Materials in Nuclear Power systems – Water Reactors*, pp. 2189-2201, 2011

Characteristic radiation induced defects

- Black spot damage
- Dislocation loops
- Nanoscale cavity formation
- Radiation-induced segregation/solute clustering
- Radiation-induced precipitation
- Transmutation effects

Introduction

- Characteristic radiation defects :
  - **Dislocation structures** (Frank faulted dislocation loops, stacking fault tetrahedra, dislocation network)
  - **Cavities** (voids and bubbles)
  - **Fine-scaled radiation-induced precipitates**. In addition, "black-dot" defects, represent indefinably small Frank loops, precipitates, or point-defect clusters

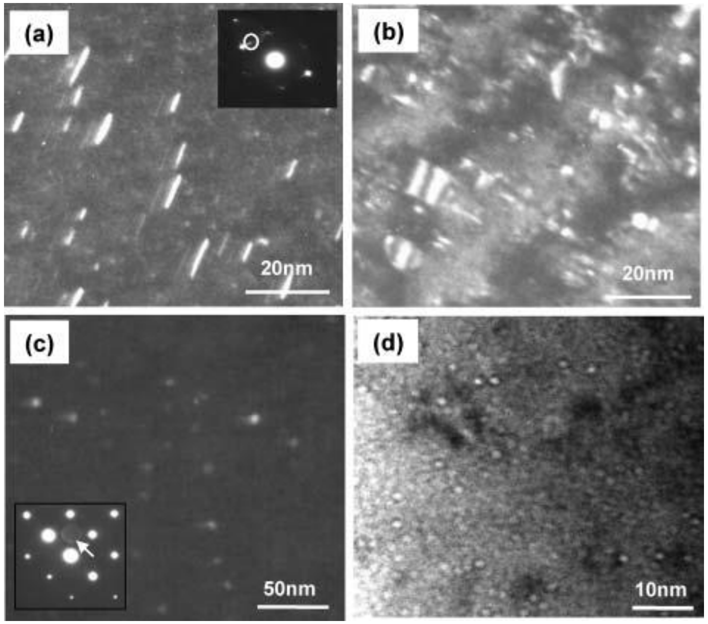

TEM images showing microstructural features observed in CW type 316 SSs PWR-irradiated to 53 dpa: (a) rel-rod dark field image of dislocation loops; (b) dark field image of dislocation loops and black dots; (c) dark field image of Ni3Si precipitates; and (d) defocused image of bubbles [Fukuya K, Fujii K, Nishioka M, Kitsunai Y. Evolution of microstructure and microchemistry in cold-worked 316 stainless steels under PWR irradiation. J Nucl Sci Technol. 2006;43:159–173.].

Frank Loops

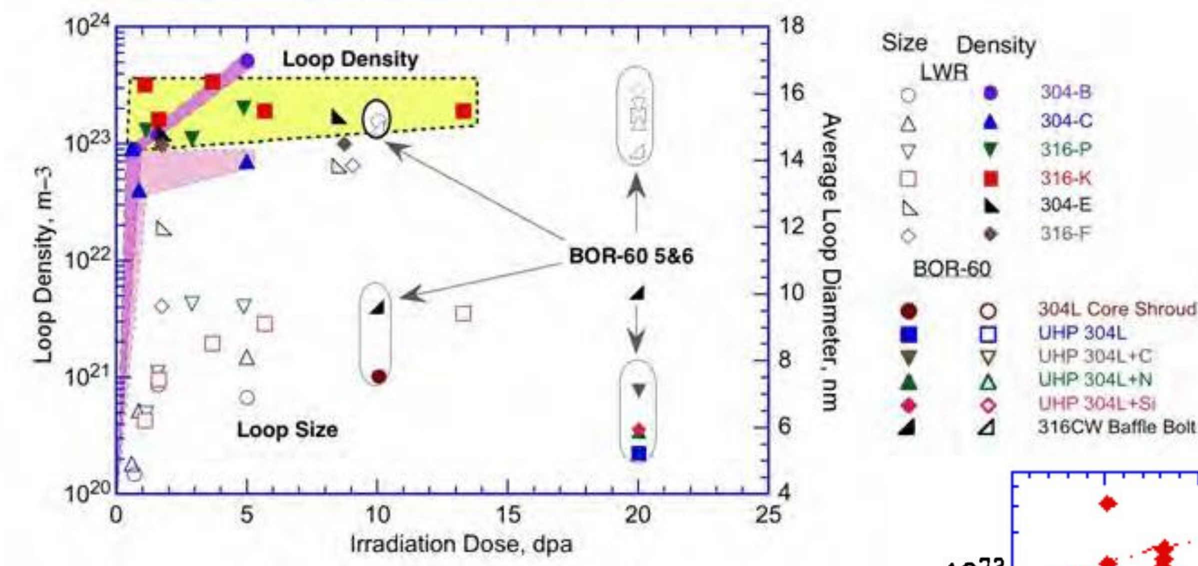

Results from the BOR-60 irradiation experiment with the data for austenitic stainless steels irradiated in a BWR [3]

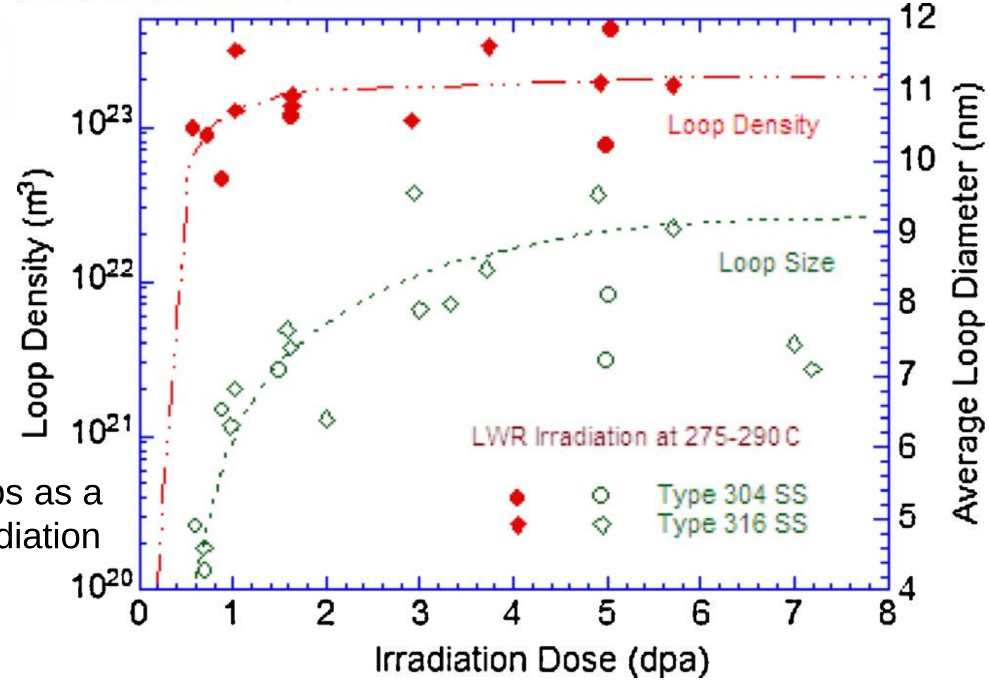

The change in density and size of interstitial loops as a function of irradiationdose (dpa) during LWR irradiation at 275–290◦C [2,4].

Cavities

Tihange baffle/former bolt as manufactured; CW 316 SS [5]

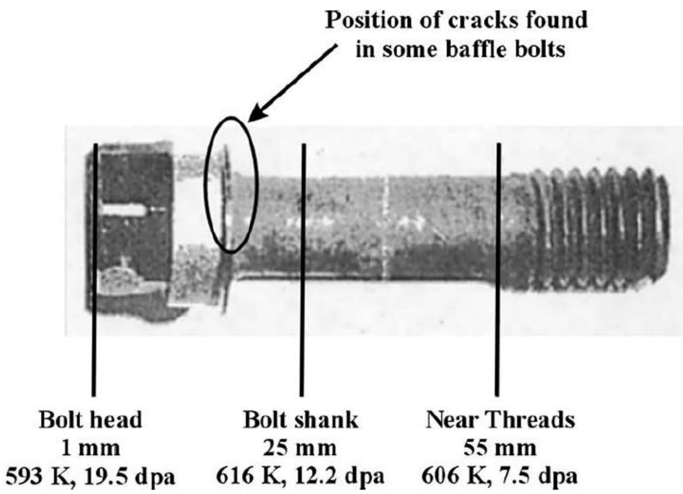

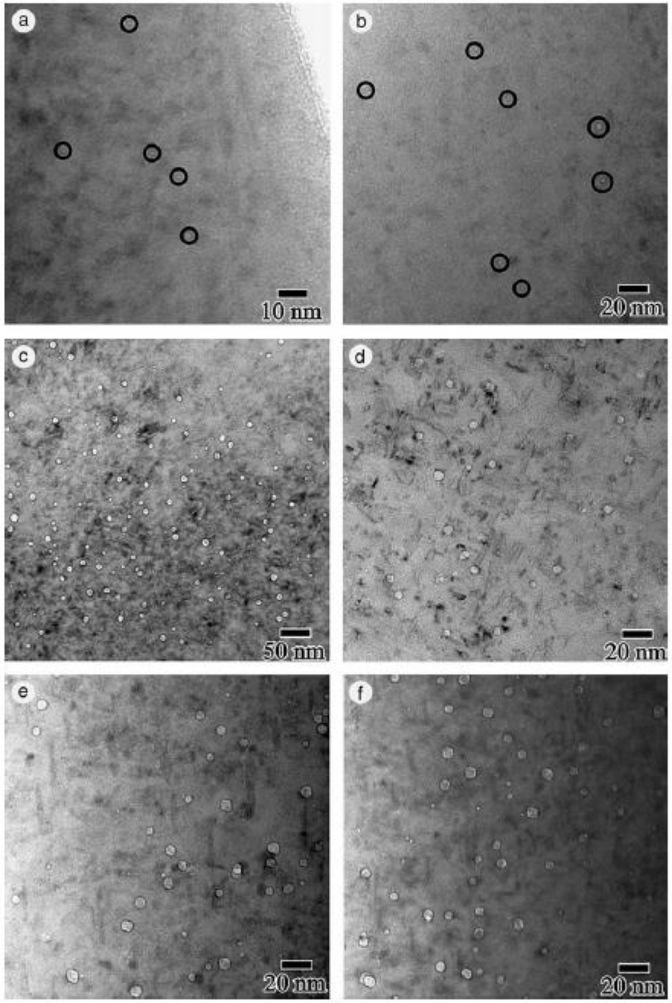

Examples are shown in (a) and (b) of the small cavities (encircled) present in a low density in the 1-mm bolt head position.
Larger cavities are present at the 25-mm position as shown in (c) and (d),and at the 55-mm position as shown in (e) and (f). The level of
swelling in the bolt head was estimated to be less than 0.01%,and up to 0.2% in the two shank positions

Radiation Induced Segregation

- 304 stainless steel irradiated to 1.7 dpa ($2x10^{22}$ n/cm2) (E > 1 MeV)) at 288 C

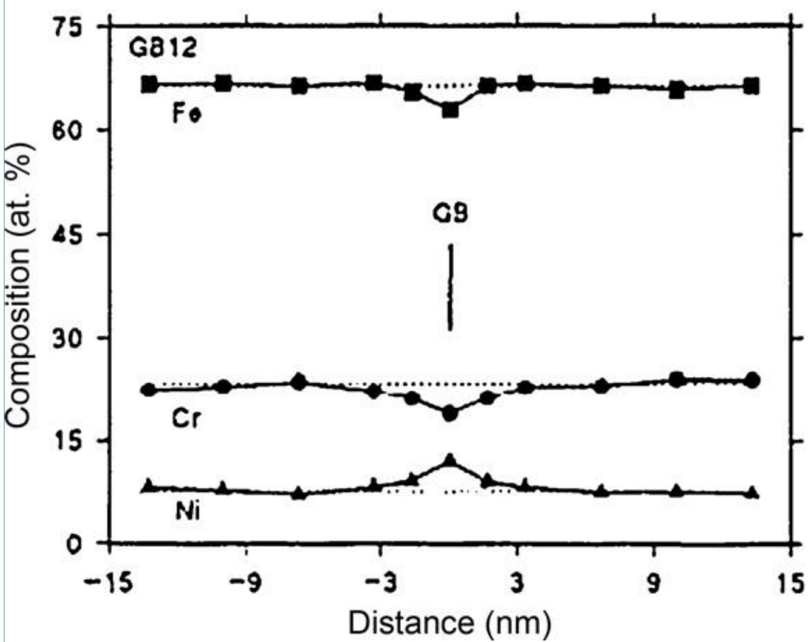

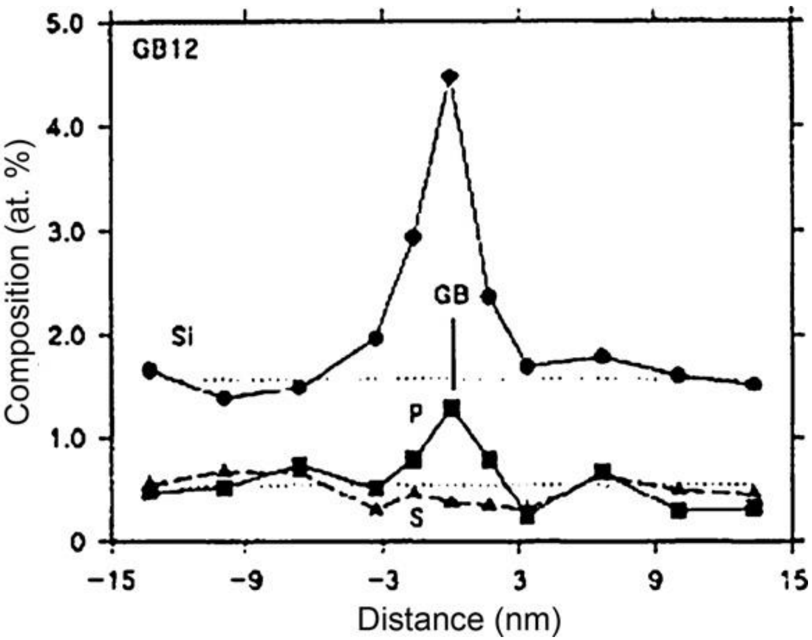

Conventional (V-shaped) grain boundary RIS profiles for a commercial purity 304 stainless steel neutron irradiated at 288 8C to 1.7 dpa [34]. Note depletion of iron and chromium at the boundary and enrichment of nickel, silicon and phosphorus[6]

Radiation Induced Segregation

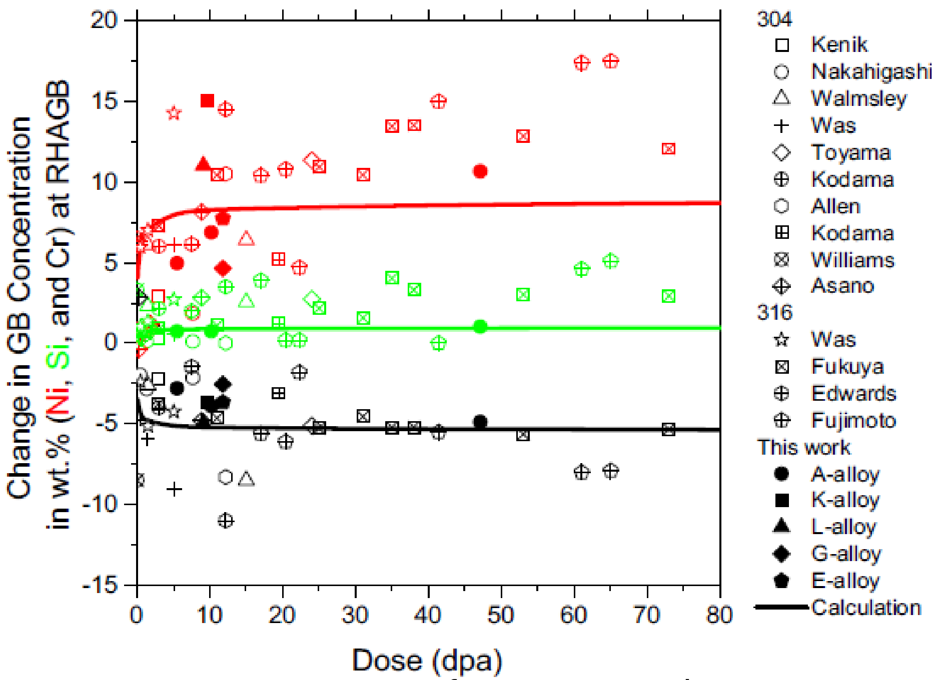

BOR-60 reactor at 320C for up to 47.1 dpa at a displacement rate of 8 x10^{-7} dpa/s [7]

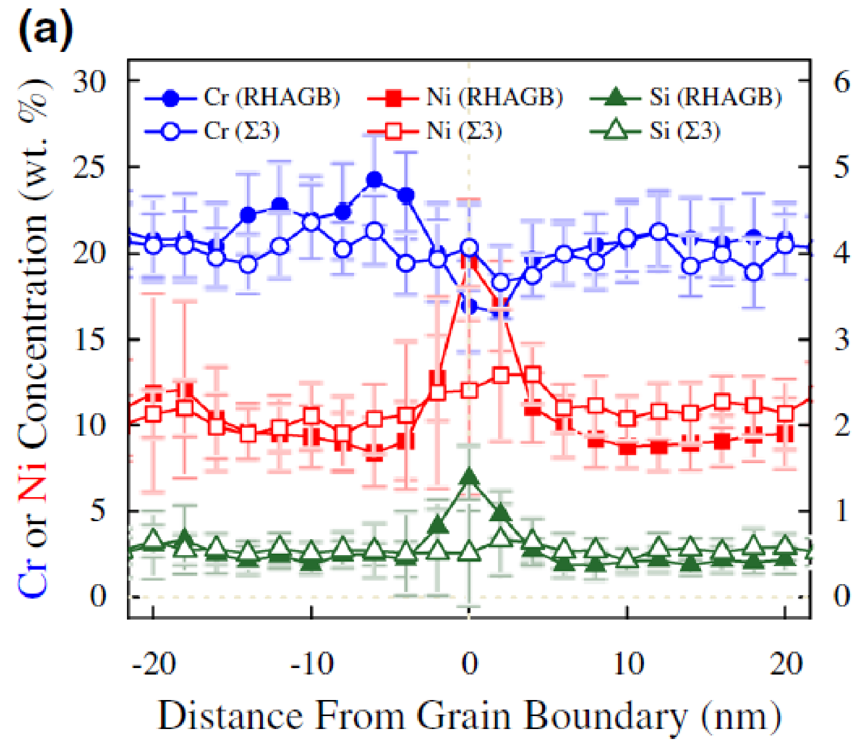

One-dimensional concentration profiles from random high-angle grain boundaries in the 47.1 dpa—irradiated specimen [7]

Radiation Induced Precipitates

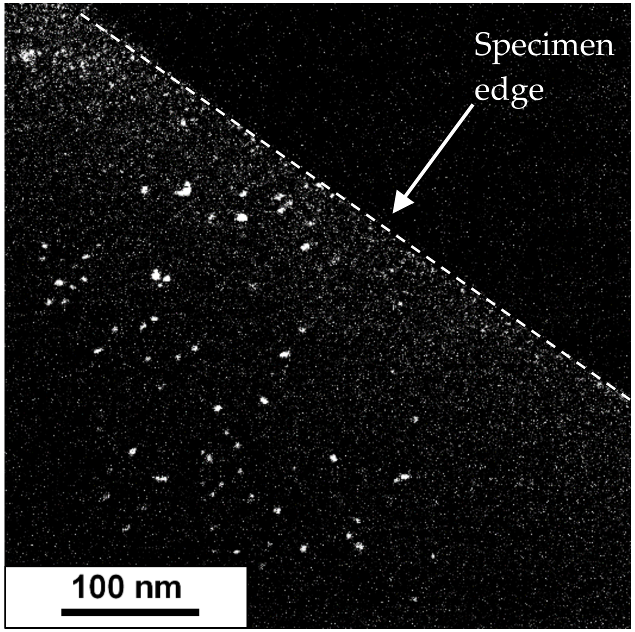

Figure 16. RIP in rel-rod DF micrograph (mixed spectrum).

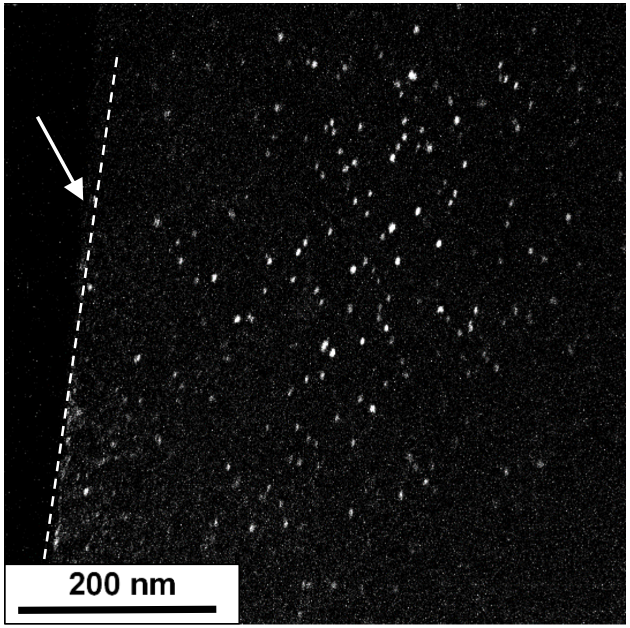

Figure 18. RIP in rel-rod DF micrograph (fast spectrum).

- ❑ CW 316 Austenitic Stainless Steel, 300C, 15 dpa
- ❑ The radiation-induced precipitates (RIP), described as a nickel and silicon rich-phases, γ' (Ni_3Si), with fcc structure

Ref: P. Bublikova Fontevraud 2018

SOTERIA related work

- **RPV internals (austenitic stainless steels) -** Task 2.1.2
  - To characterise the effect of **neutron flux** on radiation-induced microstructure
  - To study the **evolution of the microstructure** with neutron fluence including their role on fracture

Materials: Reactor vessel internals

VVER-440 Nord /Greifswald Unit 1 Internal components – Ti stabilized austenitic steels
Service 15 years , neutron flux <u>1-1.5x10^{-8} dpa/s</u>, high temperature, <u>demineralized water Without Oxygen</u>

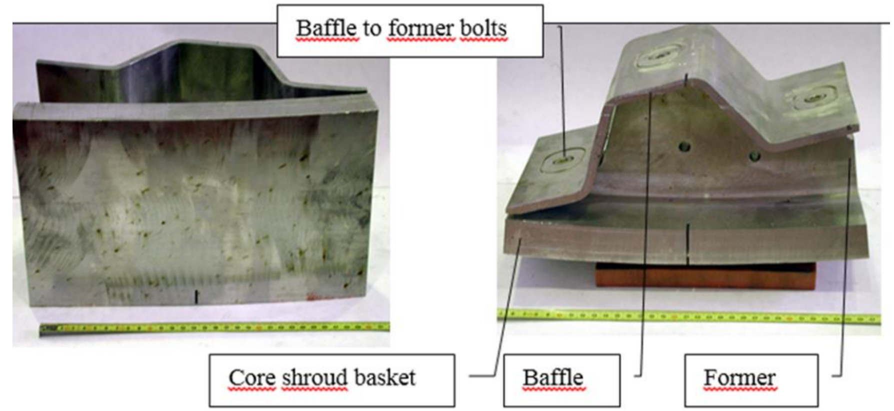

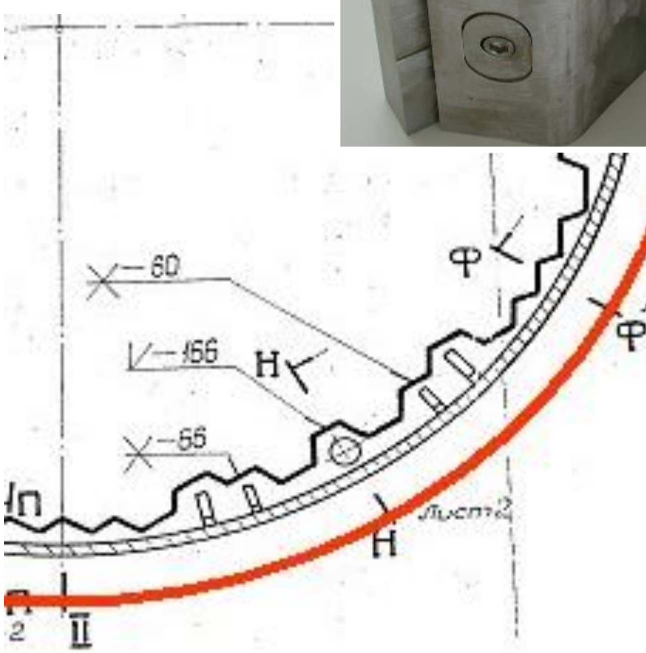

Steel	**18Cr-10Ni-Ti**
Component	**Core basket (rolled plate 32 mm)**
Microhardness	**363 ± 9**
Grain size	**40** µm
δ ferrite	**1 %**
Irradiation T	**320** °C
Dose	**5.2 dpa**
Irradiation time	**15 FPPY**

In-service irradiated WWER reactor internals material

Austenitic Stainless Steel 08Ch18N10T

C	Mn	Si	P	S	Cr	Ni	Ti	Cu	Co	N
0.07	1.41	0.45	0.011	0.007	18.18	9.72	0.49	0.03	0.02	0.013

Different microstructures and irradiation conditions

Components 15 FPY in-service irradiated	2.4 dpa	5.2 dpa	11.4 dpa	11.4 dpa
	Core barrel	Core basket	Baffle	Baffle Bolt
	Plate 36 mm	Plate 32 mm	Sheet 8 mm	M12 x 29 mm
Microhardness	285 ± 33	363 ± 9	431 ± 72	431 ± 72

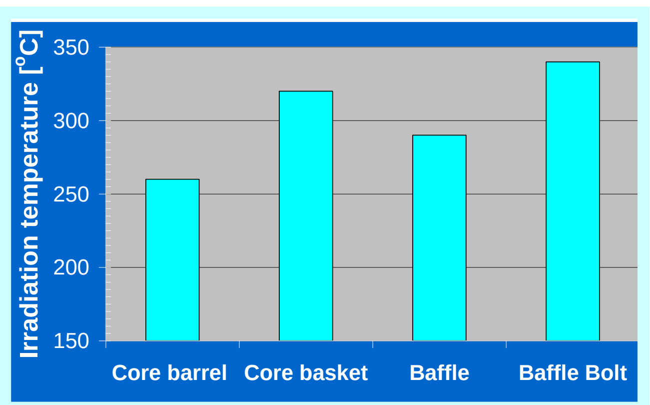

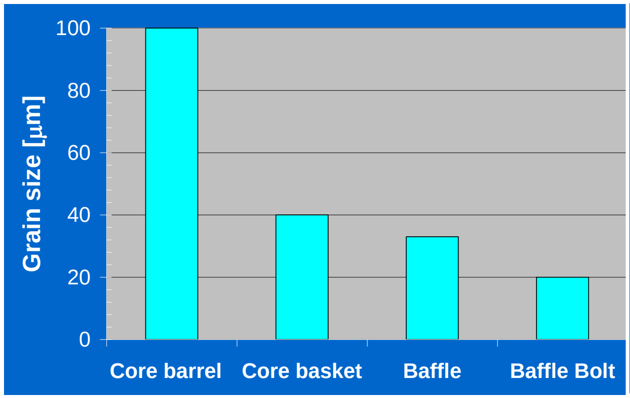

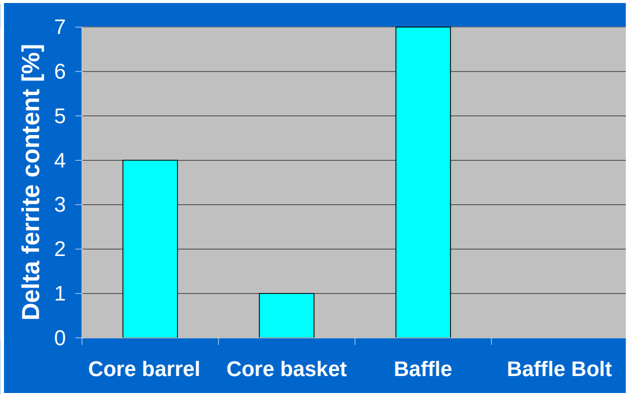

Concept of IASCC of Ti stabilized Austenitic Stainless Steel of WWER Reactor Core Internals, A. Hojna, J. Michalicka, ICG-EAC 2014, Prague

Results

08Ch18N10T (A321 analogical steel), neutron irradiated steel in VVER reactor

Core basket 5.2 dpa

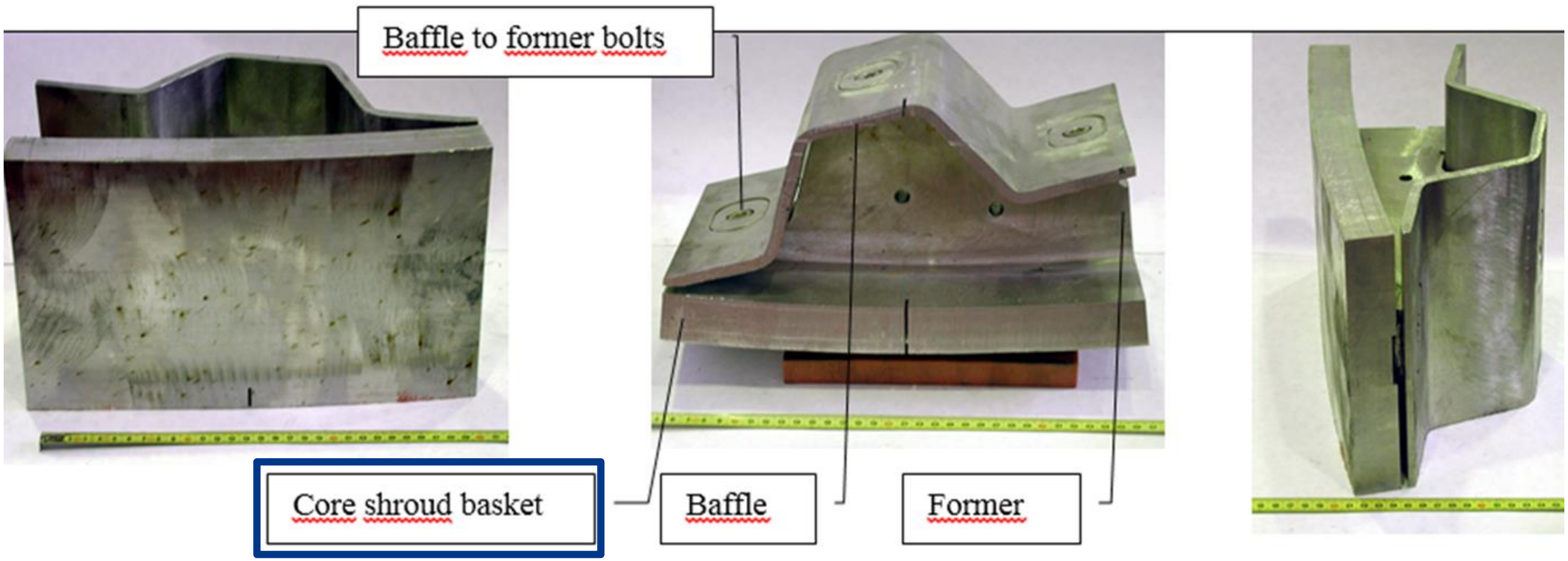

Specimen Geometry

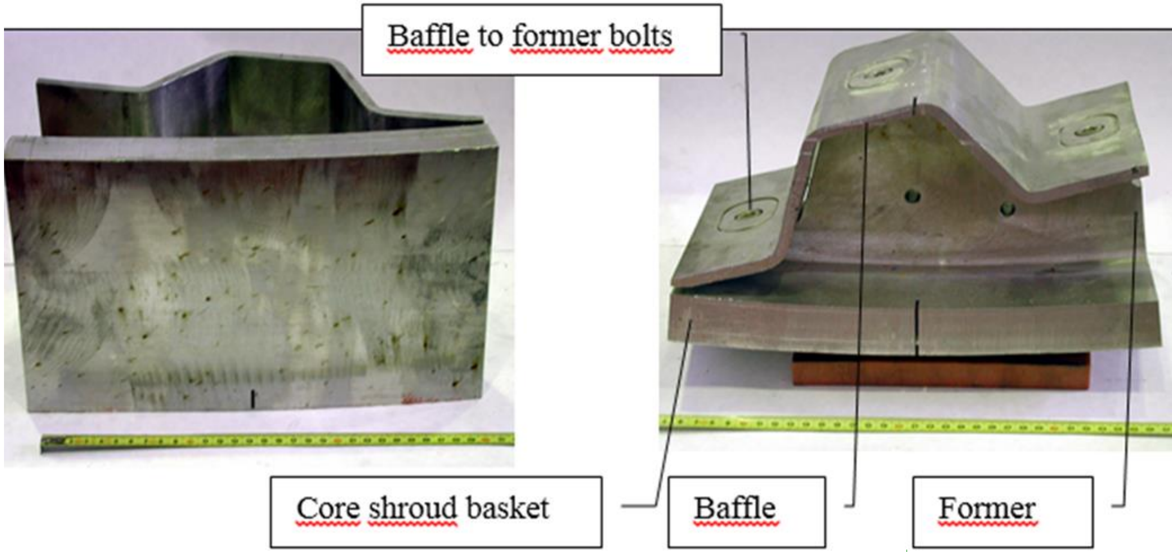

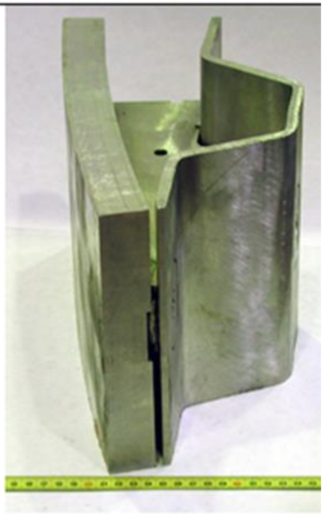

SSRT specimen

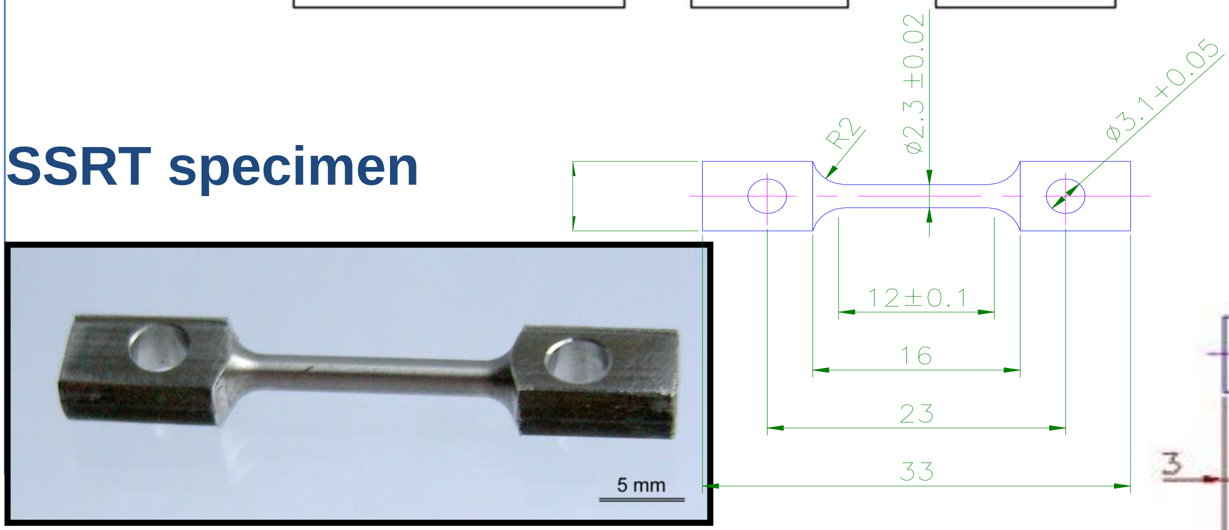

TT specimen

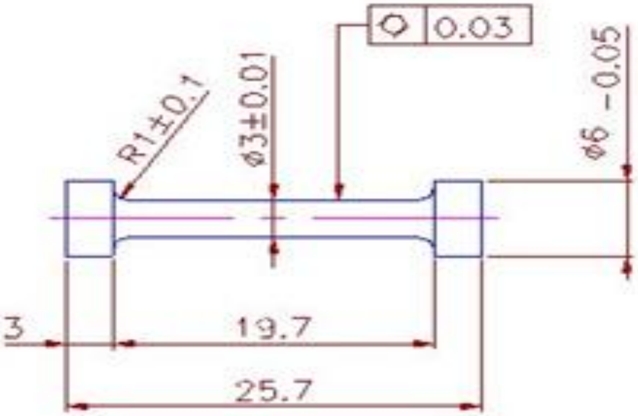

TEM Specimen Preparation

- Metallography and Twin-jet electropolishing
- Dimple Grindiner to <~ 20 μm thickness + twin-jet electropolish
- FIB milling

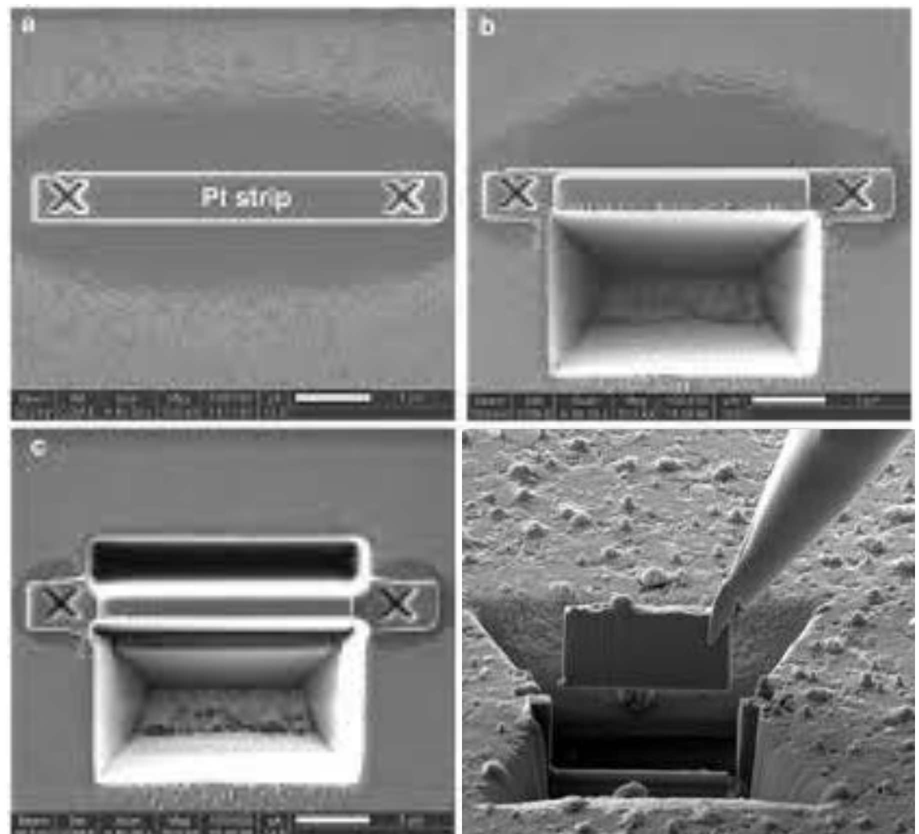

ACTIVE foils preparation for TEM Analysis

Semi-hot cell Sample cutting

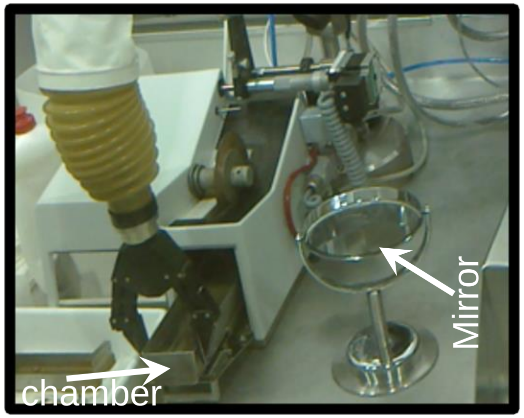

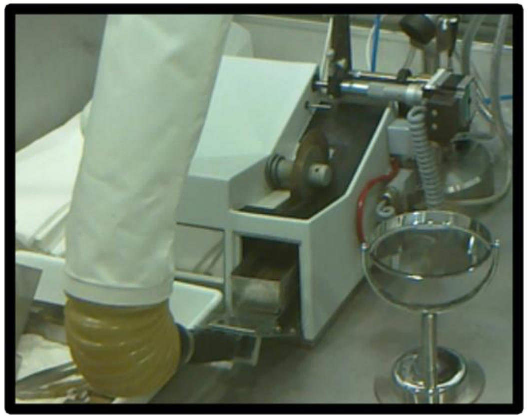

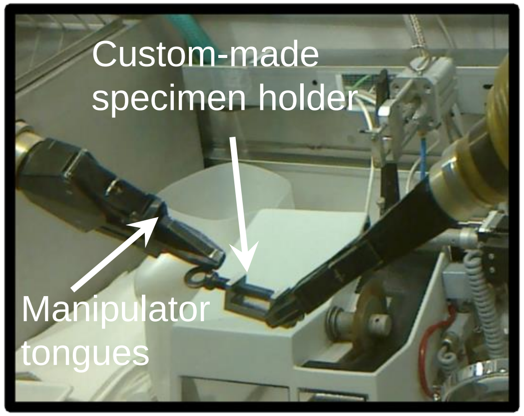

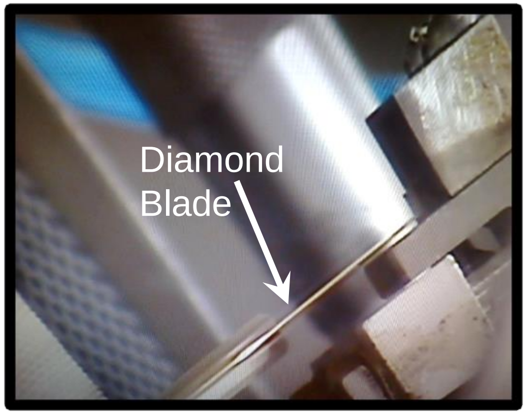

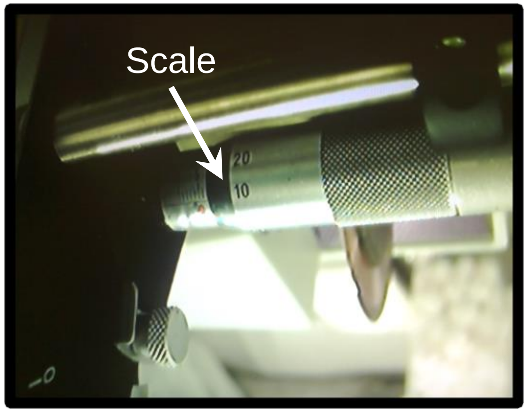

ACTIVE foils preparation for TEM Analysis


Step 1

Step 2: Grinding
1. Rough grinding
2. Fine grinding

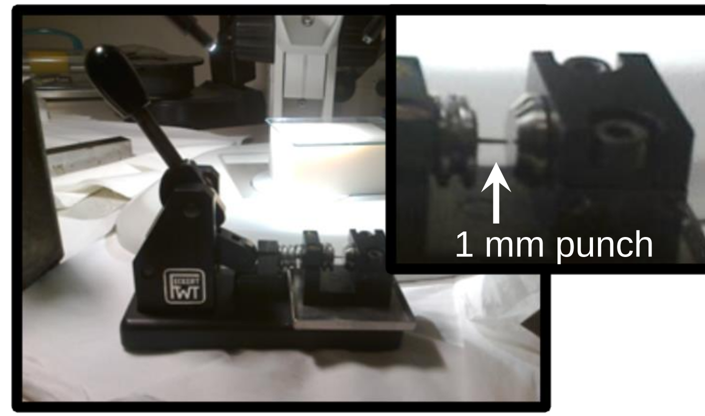

Step 3

Fischionne twin-jet

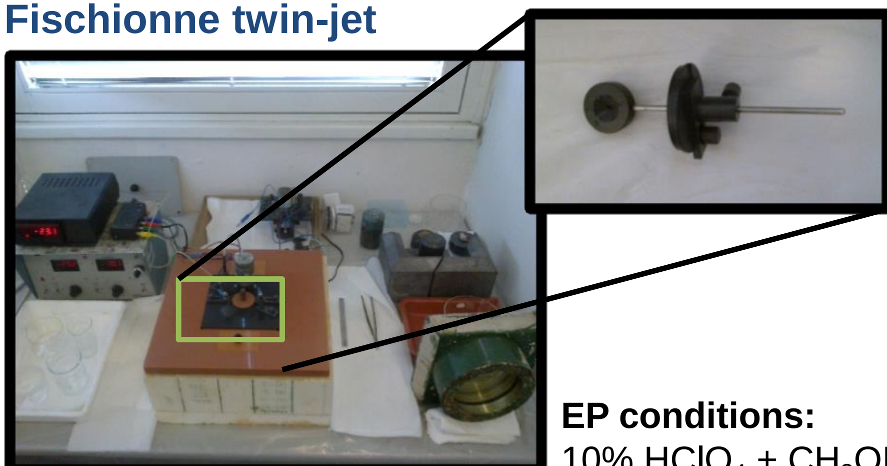
Step 4

EP conditions:
10% $HClO_4$ + CH_3OH
Voltage: 12 V
Temperature :approx. – 37°C

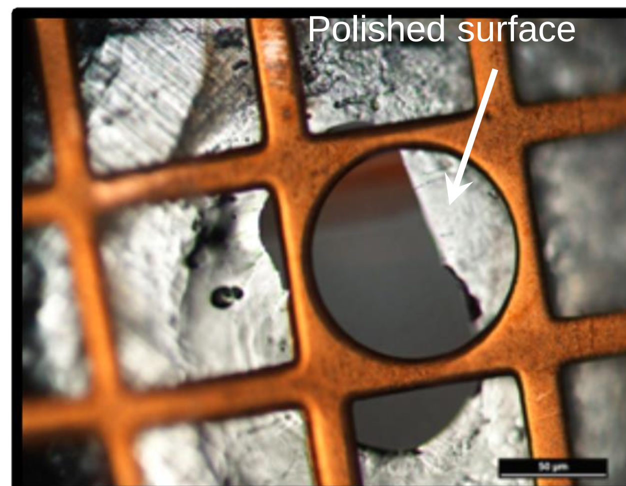

Step 5

Scientific Benefits of Applied Methodology

- Reduced the radioactivity of TEM foil **to minimum**.
- Crucial for **EDX chemical analysis** and to **increase EDX detector life-time**.

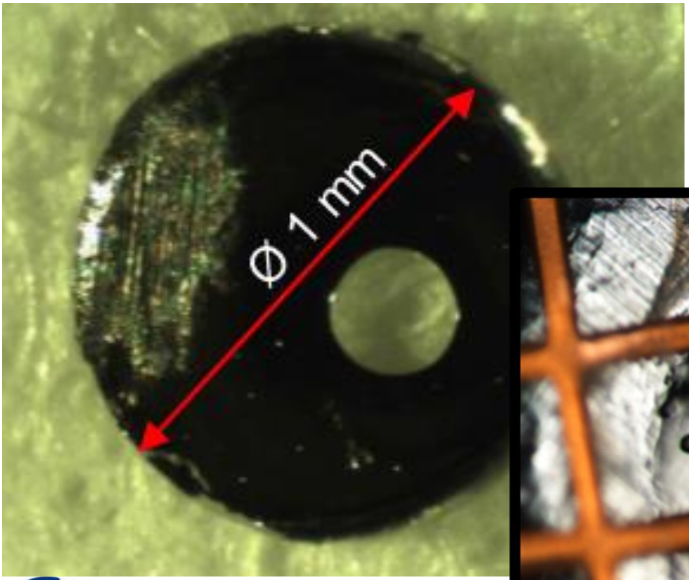

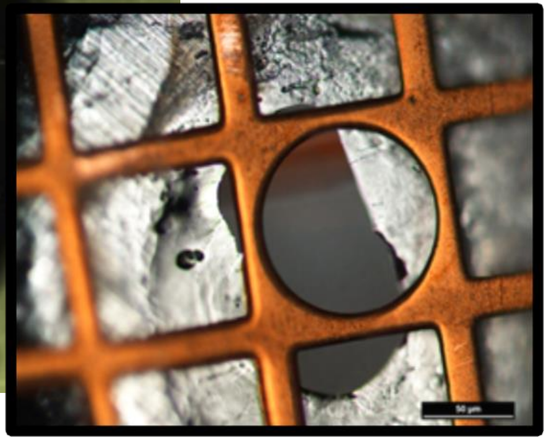

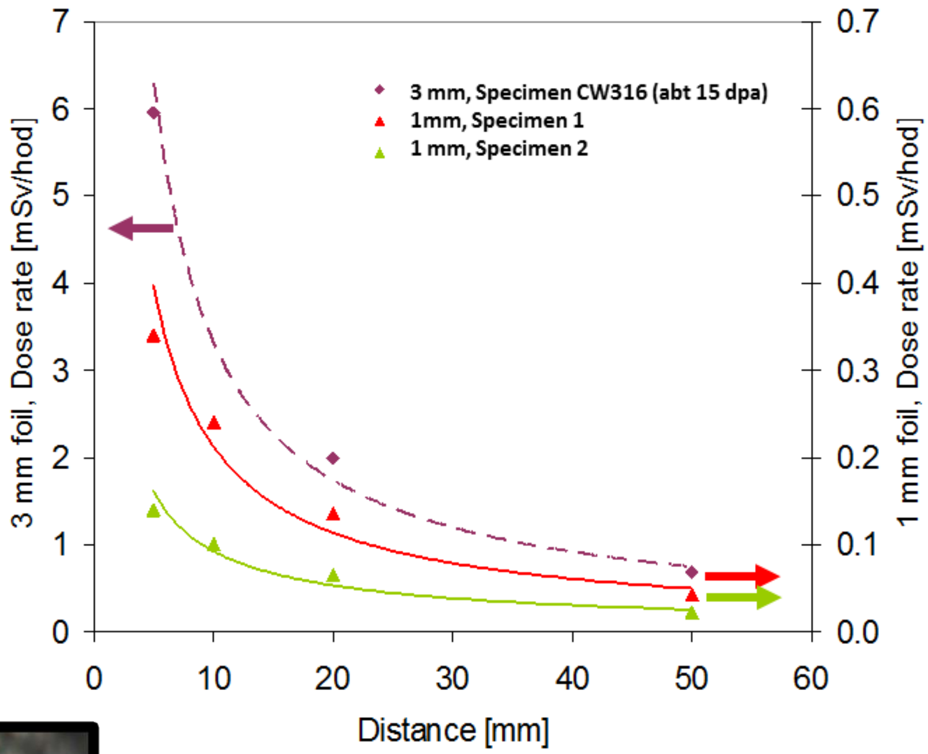

Figure: Dose rate from classical [3 mm] and currently developed [1 mm] TEM foils

Test specimen drawings with dimensions

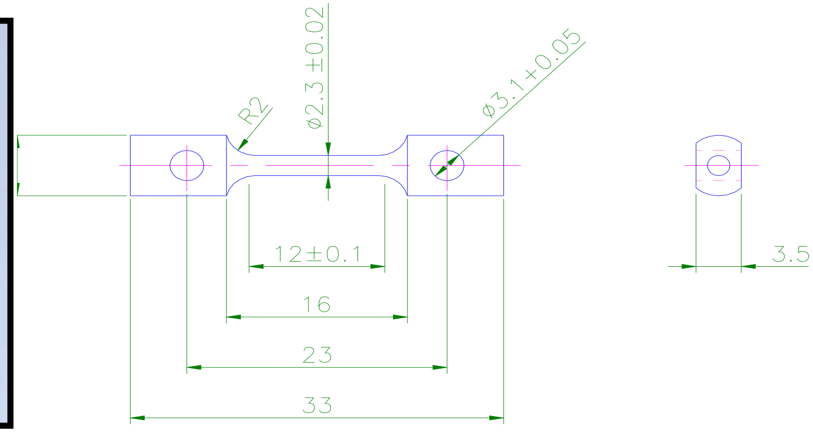

SSRT specimen broken

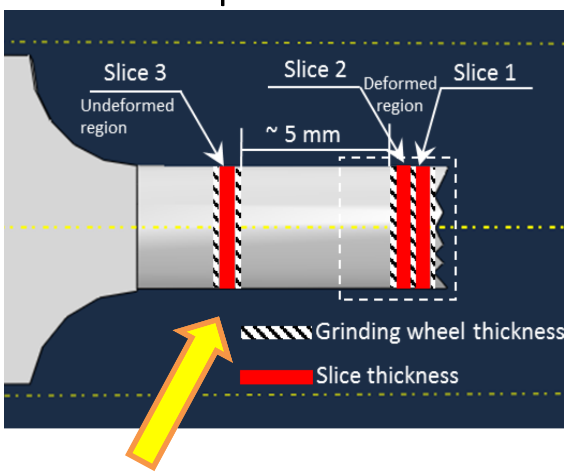

For in-service irradiation damage analysis

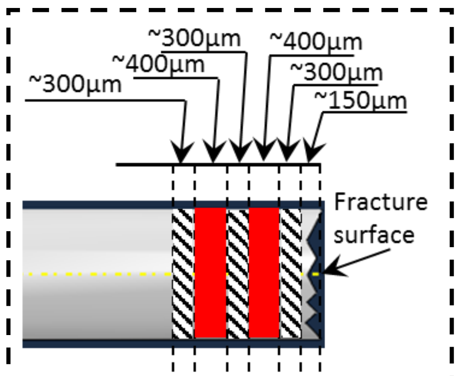

Preparation of TEM foils

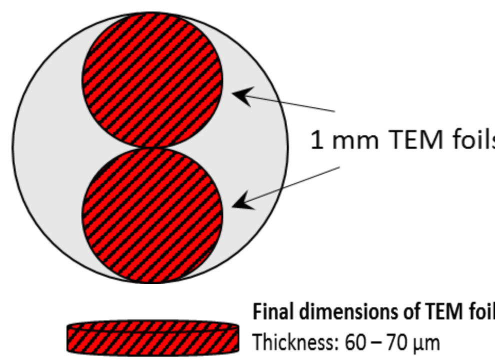

High Resolution Scanning Transmission Electron Microscope (HR-STEM), JEOL JEM 2200FS

Main parameters and modes

- Electron source: Field Emission Gun (FEG)
- Accelerating voltage: 200 kV
- In-column Omega filter
- CTEM, STEM
- HAADF STEM detector for Z-contrast imaging
- EDX detector 80 mm2
- EELS
- Electron Energy Filtering EFTEM for high contrast,
  high resolution and chemical analysis

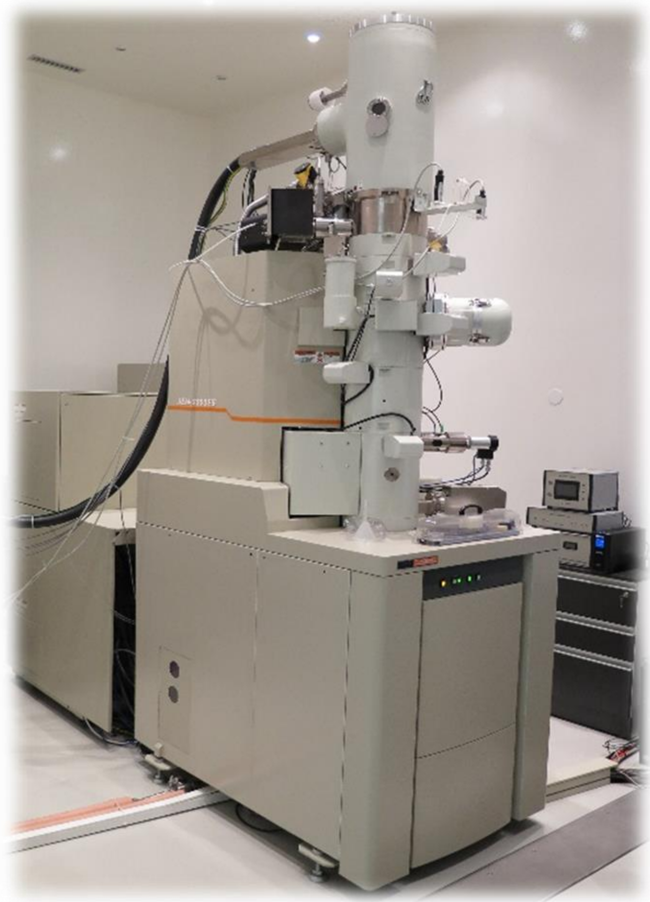

1. To characterise the effect of **neutron flux** on radiation-induced microstructure

- ❑ Frank loops
- ❑ Cavities (voids/bubbles)
- ❑ Redistribution of solutes:
  - Radiation Induced Segregation (RIS): From grain boundaries causing Cr depletion or to grain boundaries causing Ni, Si enrichment
  - Precipitation (RIP)

TEM examination of defects

TEM Results: Radiation damage

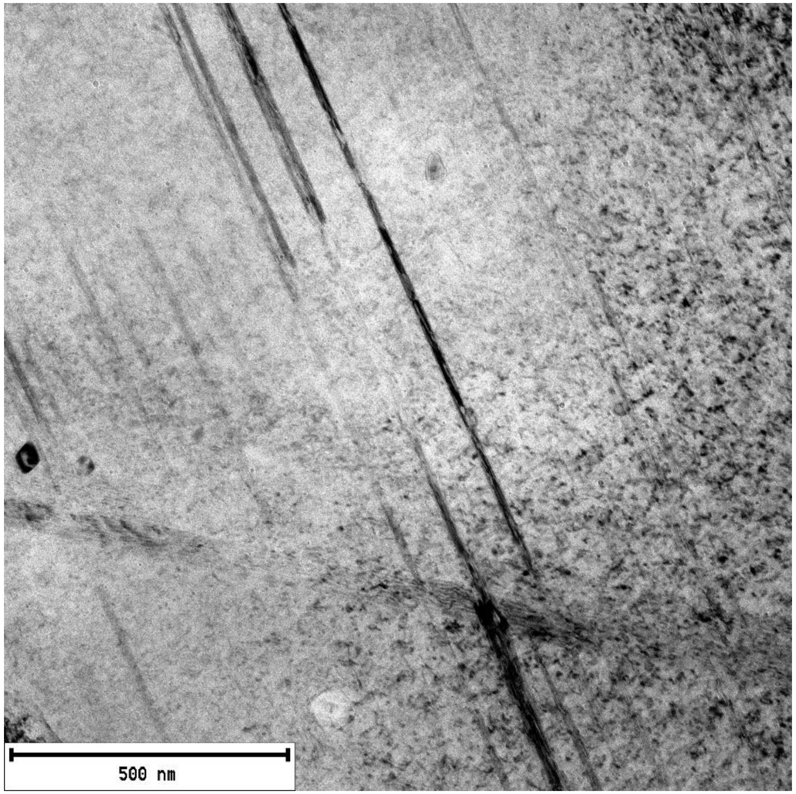

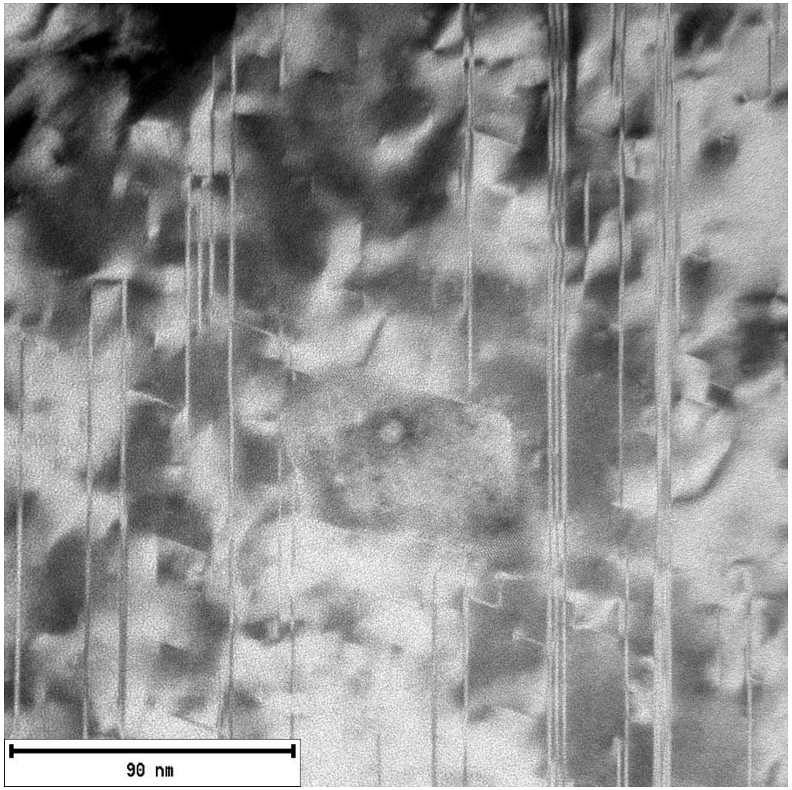

- The radiation-induced microstructure has been characterized qualitatively and quantitatively
- Characteristic radiation-induced defects were observed in all samples.

Radiation damage_Frank Loops

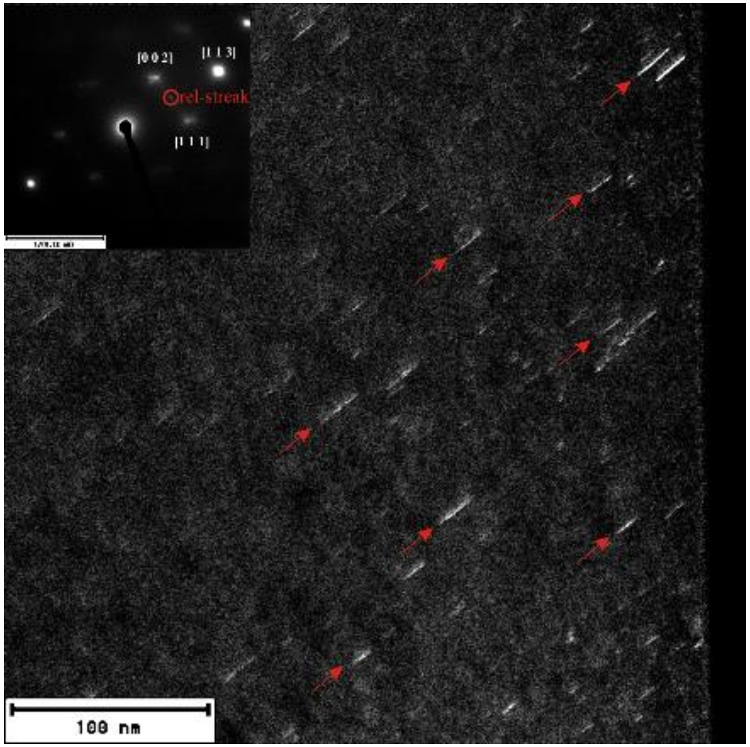

Frank loops marked by red arrows; the applied diffraction is shown in the small left corner frame.

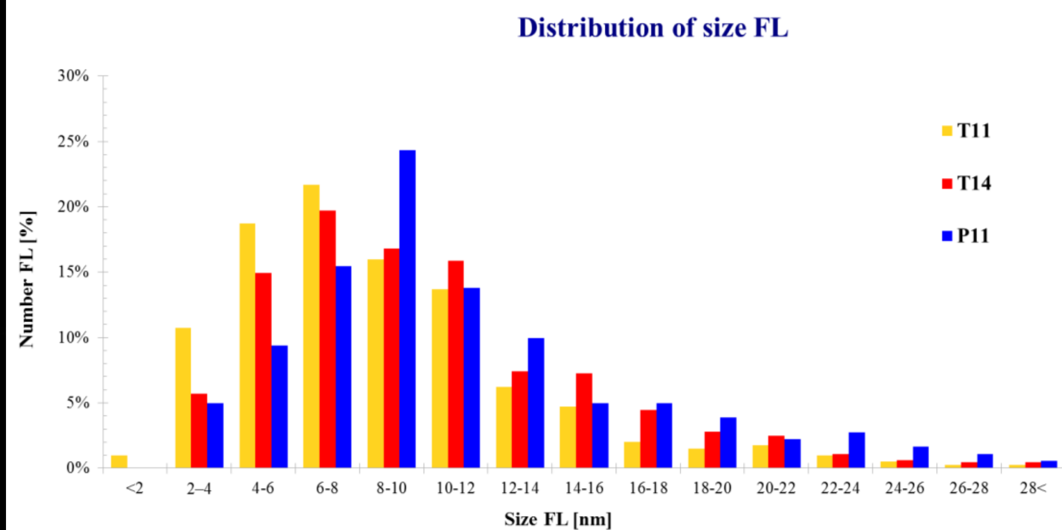

Frank loops
Average size
≈ 12.0 ± 5.0 nm
Density
≈ 8.1 ± 0.9 ×1021 m-3

Radiation damage_cavities

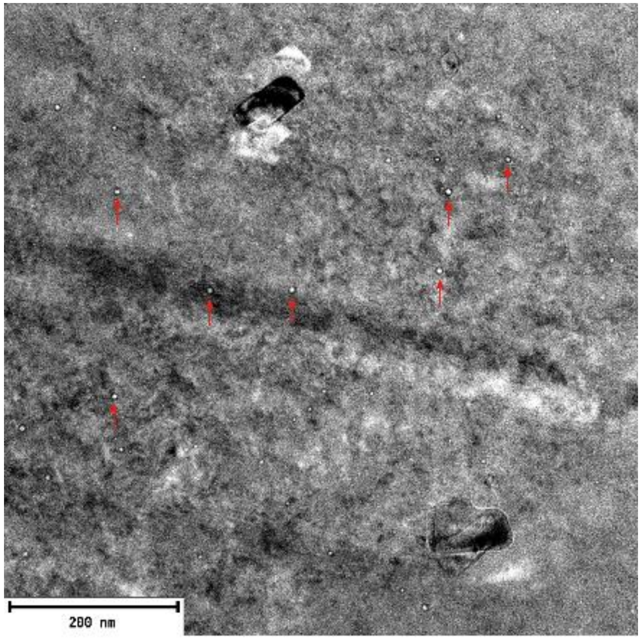

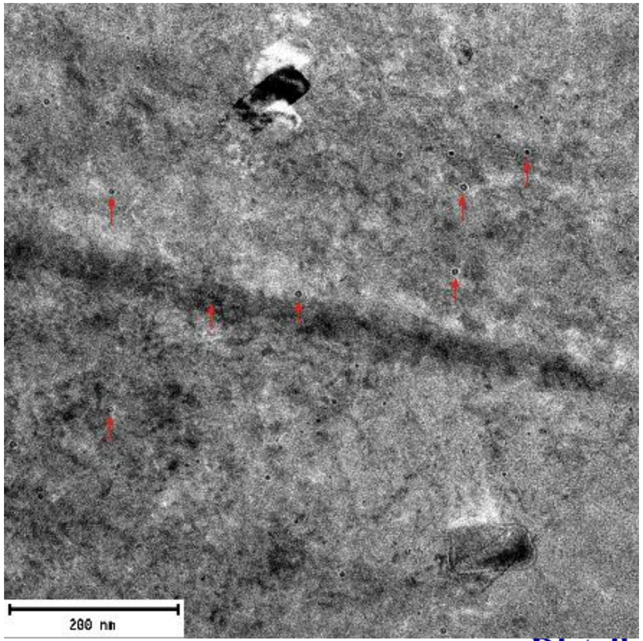

Cavities marking by red arrows: a) under-focused image, b) over-focused image

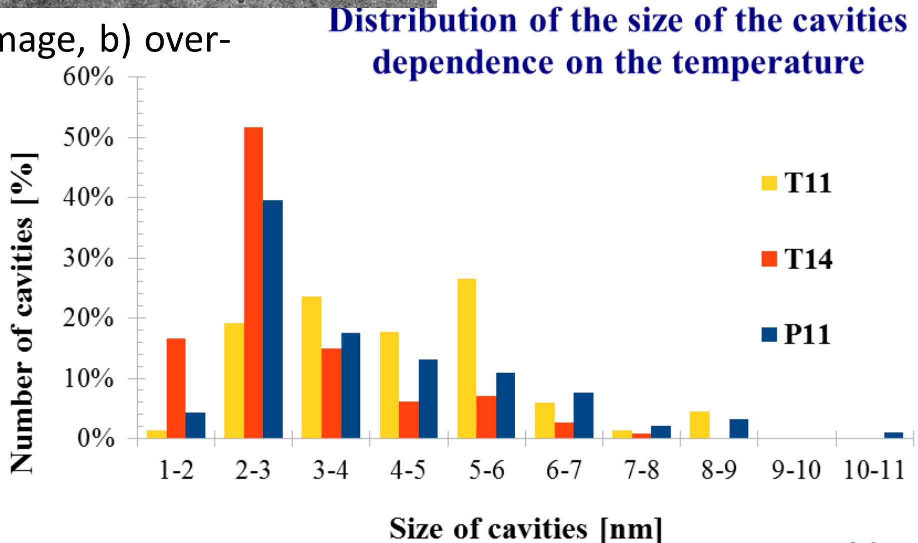

Quantitative data for the Frank loops and the cavities

Density of **Frank loops** $N_v \cdot 10^{21}$ [m^{-3}]	Average size of **Frank loops** [nm]	Density of **cavities** $N_v \cdot 10^{21}$ [m^{-3}]	Average size of **cavities** [nm]
2.8±0.2	11.9±5.0	1.7±0.3	4.4±1.5
2.7±0.3	11.8±5.8	1.7±0.2	2.9±1.2
2.7±0.1	13.4±5.3	1.7±0.1	3.9±1.9

Radiation damage_cavities

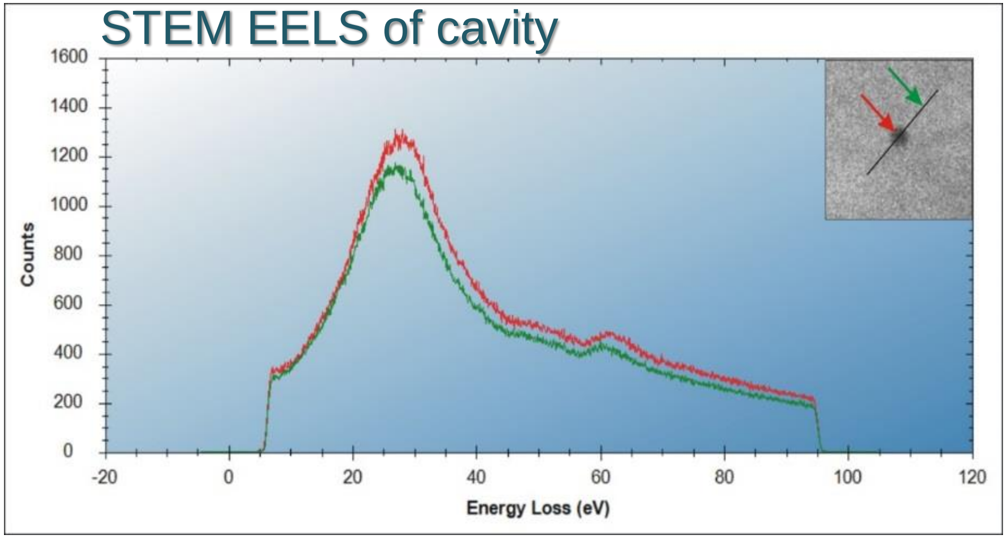

STEM EELS of cavity showing the scan line (black line) across the cavity where the EELS analysis was performed.

STEM EELS of cavity

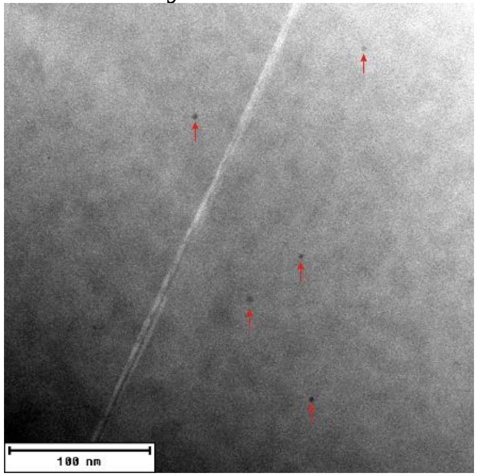

- ❑ Using the STEM EELS technique we confirmed the presence of a gas (He and/or H) in the cavities
- ❑ Both H/He gases can cause a blue shift in the plasmon peak
- ❑ The position of the plasmon peak of the cavity is shifted to the higher energy losses than the plasmon peak position of the matrix

Radiation-induced segregation

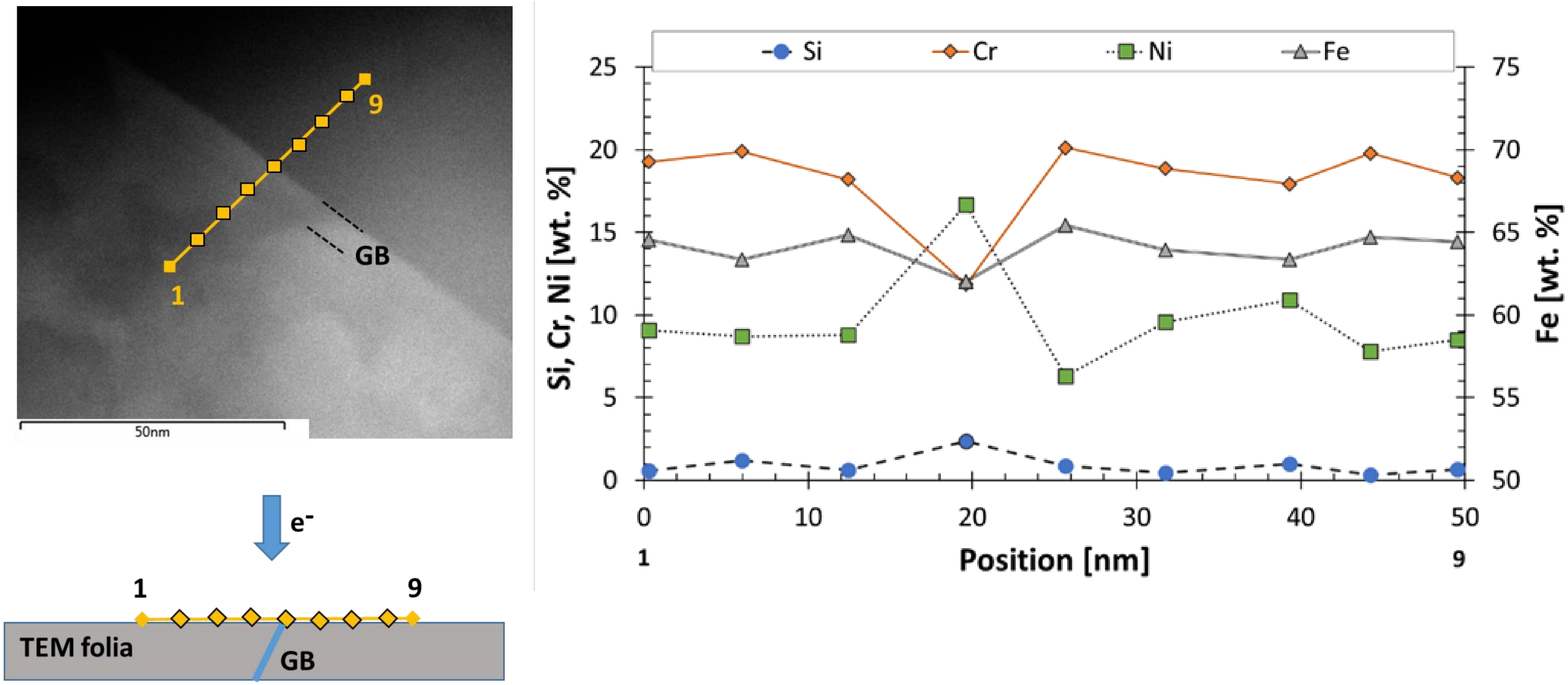

STEM EDS line scan across grain boundary; dashed line marks the position of grain boundary (GB) in the graph.

Radiation-induced segregation of Cr, Ni, Si and Mn was observed randomly across some high-angle grain boundaries using STEM EDS point analyses

Precipitates

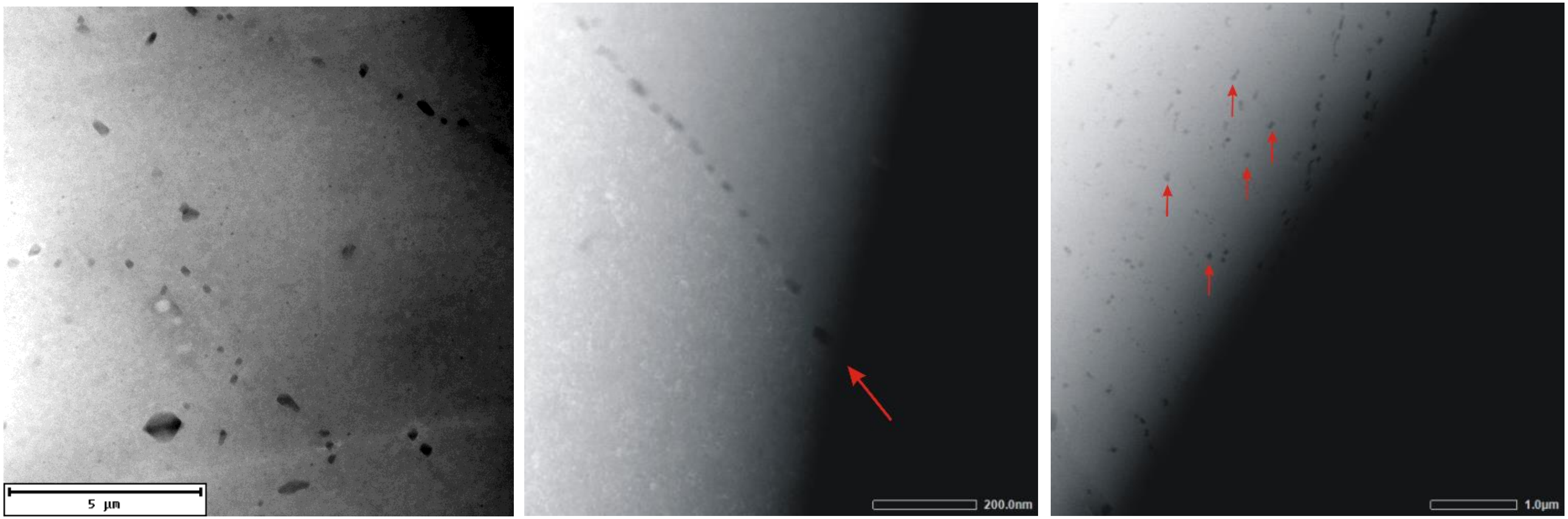

Ti-based precipitates distribution (right), decorating grain boundary of marked by red arrow (middle) and inside the austenitic grain (right), image taken in STEM mode using HAADF detector

- The precipitates were mostly Ti-based (specifically Ti and TiC).
- These precipitates belong to the original microstructure before the irradiation.
- They are distributed within the grain interiors as well as at the grain boundaries and are often arranged into chain-like structures along the grain and sub-grain boundaries

2. To study the evolution of the **microstructure** with **neutron fluence** including their **role on fracture**

- Study on the strain localization in the irradiated austenitic stainless steel under various conditions
- Specifically to address changes of microstructural interactions in
  (a) Air, 20 & 320˚C, standard & slow rates;
  (b) Air versus Water, 320˚C, slow strain rate.

In-service Irradiated specimens after tests

Fracture appearance of the selected specimens.

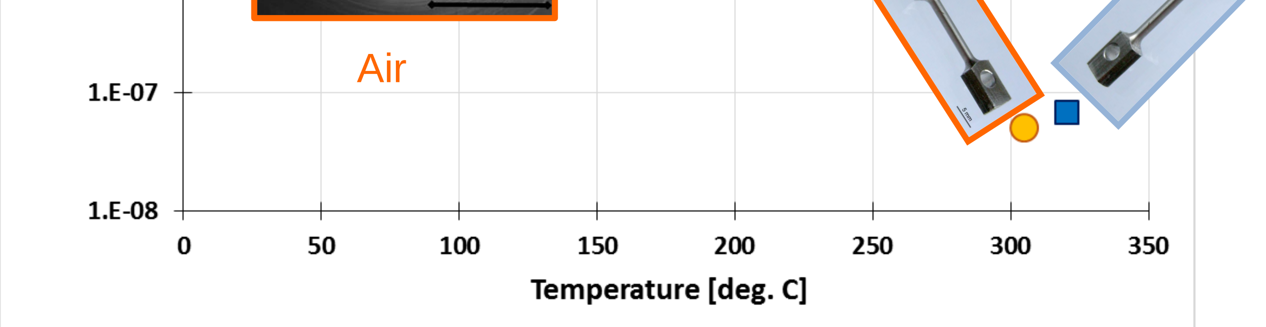

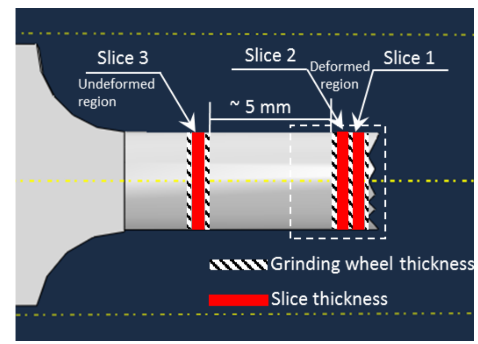

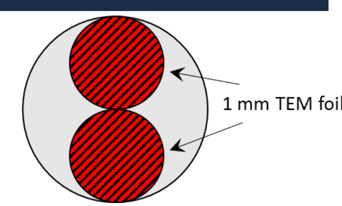

Effect of Tensile Strain on Microstructure of Irradiated Core Internal Material, basket material 08Ch18N10T austenitic stainless steel

Strain rate, temperature and water effects on deformation of neutron irradiated steel of VVER reactor core internals, A. Hojna, J. Duchon, P. Halodova, H. K. Namburi and in [8]

Strain rate & Temperature effects

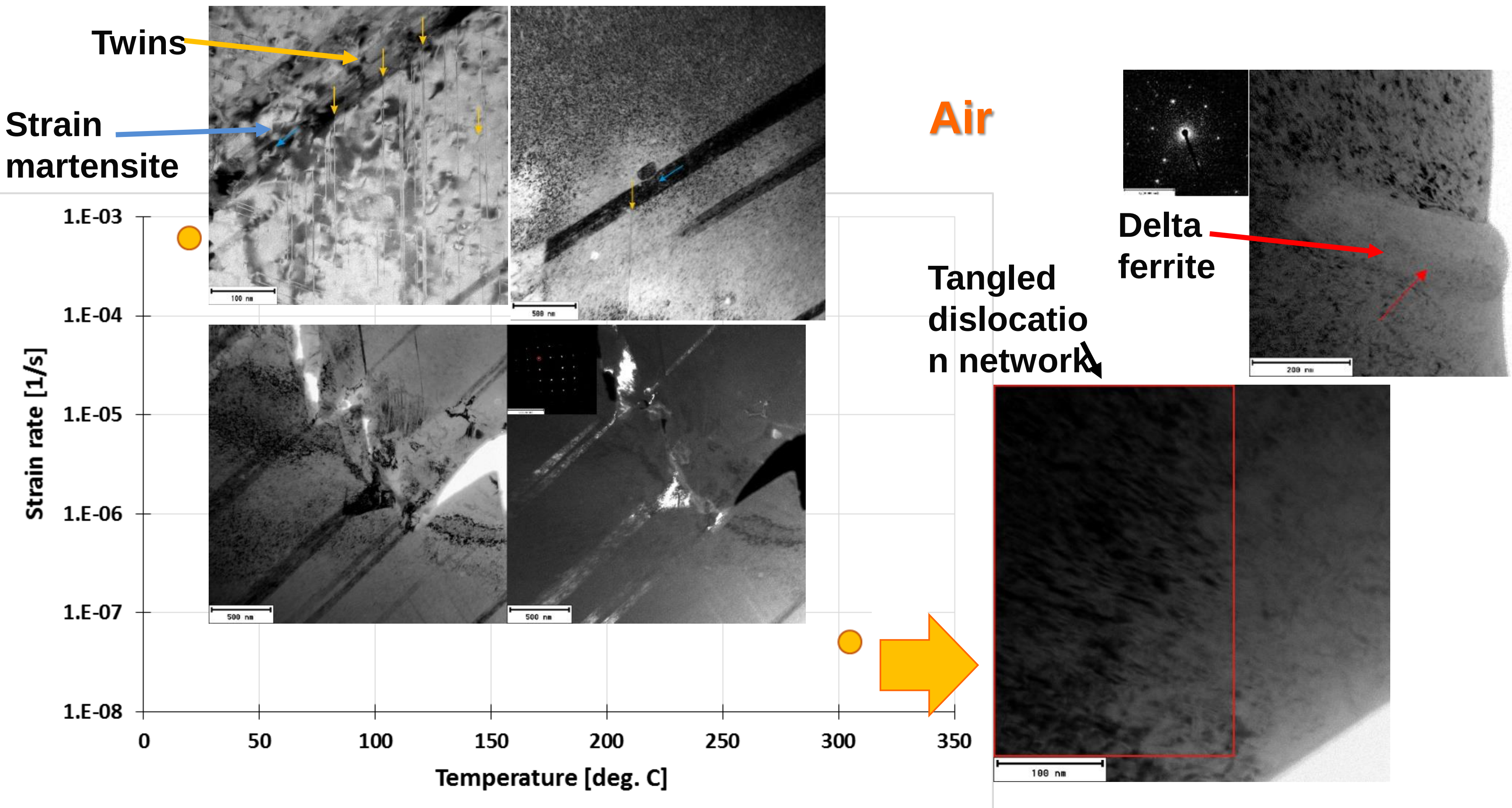

Strain rate, temperature and water effects on deformation of neutron irradiated steel of VVER reactor core internals, A. Hojna, J. Duchon, P. [illegible]odova, H. K. Namburi

Environment effect

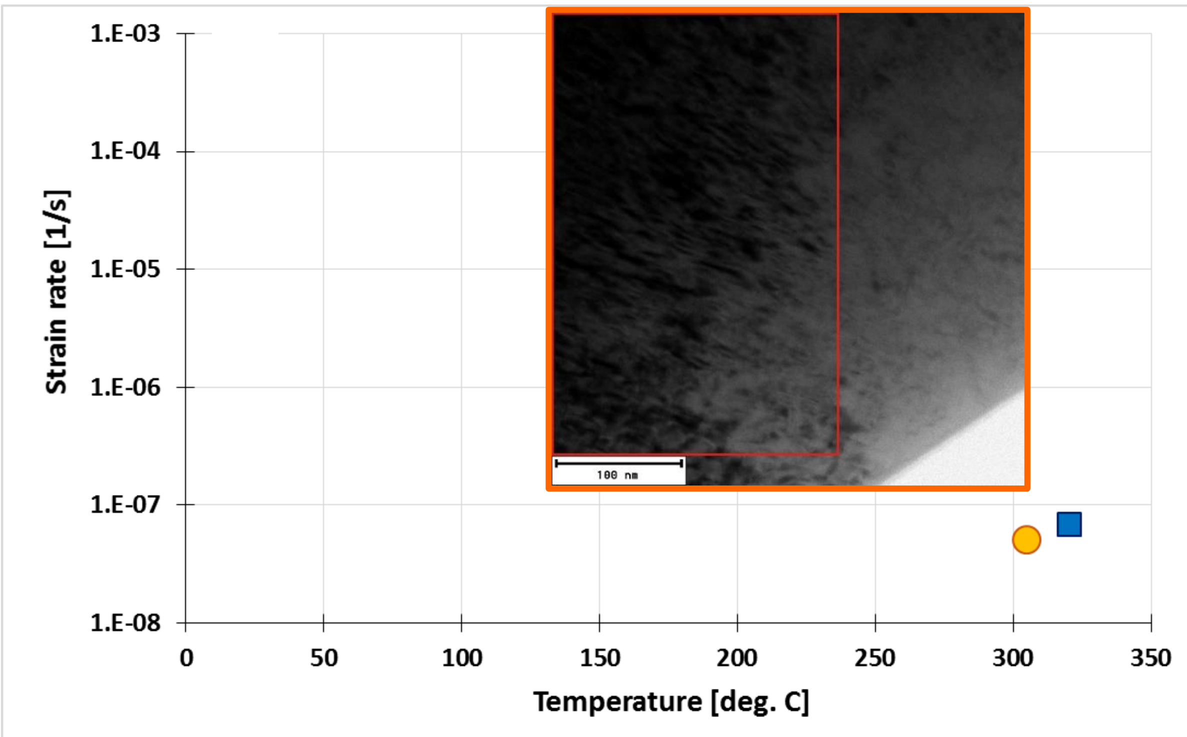

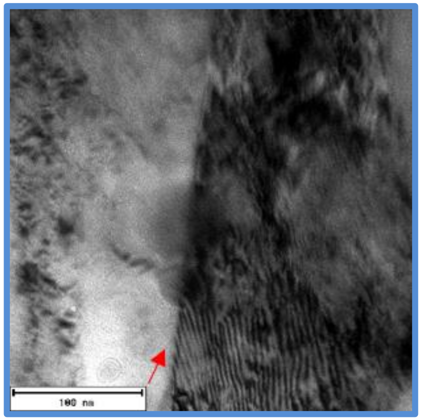

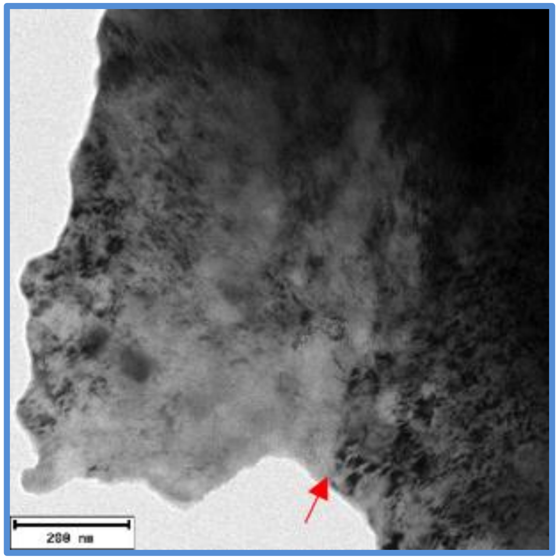

Strain rate, temperature and water effects on deformation of neutron irradiated steel of VVER reactor core internals, A. Hojna, J. Duchon, P. Halodova, H. K. Namburi

Conclusions

- Radiation damage at 5.2 dpa
  - Frank loops average size and density, RIS on grain boundaries and the cavities average size and density.
- Twinning & strain martensite areas - the deformation mechanism in the standard strain rate tensile test at RT.
- Post SSRT - the deformation mechanism characterized by presence of tangled dislocation network without dislocation channels.
- No effect of the water environment on the deformation structures was observed.

Strain rate, temperature and water effects on deformation of neutron irradiated steel of VVER reactor core internals, A. Hojna, J. Duchon, P. Halodova, H. K. Namburi

Future Steps

- **TEM observation of**
  - specimens of the baffle (11.2 dpa)/ Bolt (11.4) and/or Barrel (2.4 dpa)
  - specimens irradiated in BOR-60
- **Ion Irradiations of Reference material**
  - Ion beam facility at HZDR
  - 2.5 dpa reached at two different fluxes (about 10^{-5} dpa/s and 10^{-3} dpa/s)
- Further step: assess stability of radiation induced features produced under different flux conditions by in-situ annealing at the interior of a TEM
- Conclusions on a flux effect of the steel

JAN DUCHON (CVR)
PATRICIE HALODOVA (CVR)
ANNA HOJNA (CVR)
PETRA BUBLIKOVA (CVR)

MERCEDES HERNÁNDEZ MAYORAL (CIEMAT)

Thank You